The Contribution of Submarine Optical Fiber Telecom Cables to the Monitoring of Earthquakes and Tsunamis in the NE Atlantic

👤 Luis Matias[1]*, 👤 Fernando Carrilho[2], 👤 Vasco Sá[3], 🧑 Rachid Omira[1], 🧑
Manfred Niehus[3,4], 👤 Carlos Corela[1], 👤 José Barros[5] and 👤 Yasser Omar[6]

[1]Instituto Dom Luiz, Faculdade de Ciências, Universidade de Lisboa, Lisbon, Portugal

[2]Instituto Português do Mar e da Atmosfera, Lisbon, Portugal

[3]Instituto de Telecomunicações, Physics of Informations and Quantum Technologies Group, Lisbon, Portugal

[4]Instituto Superior de Engenharia de Lisboa, Lisbon, Portugal

[5]Autoridade Nacional de Comunicações, Lisbon, Portugal

[6]Instituto Superior Técnico, Universidade de Lisboa, Lisbon, Portugal

Recent developments in optical fiber cable technology allows the use of existing and future submarine telecommunication cables to provide seismic and sea-level information. In this work we study the impact of three different technologies, 1) SMART, Science Monitoring and Reliable Telecommunications; 2) DAS, Distributed Acoustic Sensing, and; 3) LI, Laser Interferometry, for effective earthquake and tsunami monitoring capabilities on the NE Atlantic. The SW Iberia is the source area of the largest destructive earthquake that struck Europe since the year 1000, the November 1, 1755 event. This earthquake generated also a destructive tsunami affecting the whole basin. This tectonically active area is crossed by the CAM (Continent-Azores-Madeira) submarine cable on a ring configuration. Due to the end of cable lifetime the current cables need to be replaced by 2024 and the technical requirements must be defined in mid-2021. The Azores archipelago is the focus of frequent seismic crizes and occasionally destructive earthquakes. A common feature of these seismic events is that they take place offshore, an area that is difficult to monitor from land-based instruments. In this work we evaluate the

contribution of SMART cables to the earthquake monitoring and tsunami early warning system in SW Iberia and show how DAS and LI can improve earthquake monitoring on two active domains of the Azores. For tsunami early warning, we show how the offshore sea-level measurements provide clean offshore tsunami records when compared to coastal observations by tide gauges, which greatly improves the efficiency of the system. For earthquake monitoring, the data processing operational routine is examined using Monte-Carlo simulations. These take into consideration the errors in phase picking and the uncertainty on the 1D velocity model used for earthquake location. Quality of earthquake location is examined using the difference between the true location and the centroid of the computed epicenters and by the overall ellipse of uncertainty obtained from 100 runs. The added value provided by instrumented submarine telecommunication cables to mitigate earthquake and tsunami risk demonstrated in this work will help authorities and the society in general to take the political decisions required for its full implementation worldwide.

Introduction

The high capacity telecommunications between Portugal mainland, archipelagos of Madeira and Azores are sustained by three submarine cables laid as a ring, as sketched in Figure 1. Such a geometry allows for redundancy in the case of any incident occurring in one of the branches. In the Azores, the 9 Islands are also connected by unrepeatered submarine telecommunication cables, as illustrated in Figure 2. The first set of cables is known as CAM from C (Continental mainland), A (Azores) and M (Madeira).

FIGURE 1

FIGURE 1. Shaded bathymetry map of Iberia, northwest Africa and Central Atlantic (Smith and Sandwell, 1997). Solid yellow line: plate boundaries from Bird (2003). White boxes, location for Figures 2, 3. Small red circles: epicenters, from ISC, M > 4, 1964–2018, http://www.ISC.ac.uk. GC: Gulf of Cadiz; GF: Gloria

Fault; TR: Terceira Ridge; C: Mainland Portugal; A: Azores archipelago; M:
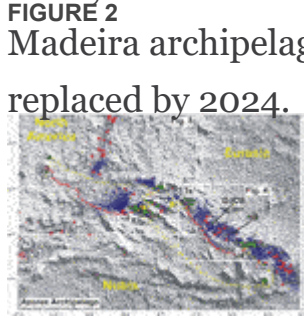Madeira archipelago. Thick blue lines show the CAM submarine cables to be replaced by 2024.

FIGURE 2

FIGURE 2. Sketch location of the submarine telecom cables in operation at the Azores archipelago (yellow and red lines) overlaying the shaded bathymetry map (Smith and Sandwell, 1997). Frame location provided on figure 1. The cables in red will be discussed in detail later in the text. White boxes for Figures 4, 5. Green triangles show the location of the land seismic stations used by IPMA for earthquake monitoring. Small blue dots: epicenters from ISC, 1960–2019, http://www.ISC.ac.uk. Red starts show the epicenters for M > 5 from ISC, 1920–2019. The large yellow stars show the location of the two most recent destructive earthquakes, the January 1, 1980 and July 9, 1998. Islands mentioned in the text, Fl – Flores, Fa – Faial, Te – Terceira, SM – S. Miguel. DJCB – D. João de Castro Bank, HB – Hirondelle Basin.

Mainland, Madeira and the Azores comprise one tectonic domain influenced by the interplay between three major tectonic plates, which is generally designated as the Azores-Gibraltar fracture zone (AGFZ). Eurasia and Nubia are colliding at a slow speed (~4–5 mm/year, e.g., Fernandes et al., 2007) S and SW Portugal mainland and slide along the Gloria Transform Fault North of Madeira. In the Azores we have a diffuse oblique spreading regime East of 30°W and a triple junction between Nubia, Eurasia and the North-American plates (Figure 1).

Earthquake and tsunami catalogues document several large events on the AGFZ, marking the western plate boundary between the Eurasian and Nubian plates. In the SW Iberia Margin (SWIM), eastern domain of the AGFZ, the largest destructive earthquake in Europe history since the year 1000, took place on November 1st, 1755 (e.g., Gutenberg and Richter, 1949; Johnston, 1996; Martinez-Solares and Lopez-Arroyo, 2004; Stucchi et al., 2013). This earthquake caused a destructive tsunami that hit the coasts of Portugal, Spain and Morocco, and reached France, England, the Caribbean and Brazil (Baptista and Miranda, 2009). The SWIM was also responsible for the most important earthquake of the 20th century that occurred on February 28th, 1969 and triggered a small tsunami that was recorded by the tide gauge networks of Portugal, Spain and Morocco (Baptista and Miranda, 2009). The central domain of the AGFZ, the Gloria Fault, although exhibiting a low seismic activity, was the place of the November 25th, 1941, largest strike-slip event ever recorded (Bird and Kagan, 2004) until the April 11, 2012 Mw 8.6 Sumatra earthquake. A small tsunami followed the 1941 earthquake with a maximum wave height of ~0.45 m recorded at Casablanca (Morocco) tide gauge station (Baptista et al., 2016). In the Azores, western domain of the AGFZ, seismic crizes are frequent and destructive earthquakes occasionally occur. The January

1st, 1980 and the July 9th, 1998 are recent examples of large earthquakes that struck the Azores (Hirn et al., 1980; Matias et al., 2007). Another major event that affected the Madeira archipelago, was the May 26th, 1975, magnitude 8.1 Ms (Kanamori and Abe, 1979), originated north of Madeira archipelago and located south of the Gloria Fault. This event generated a tsunami well recorded in Azores (~35 cm) and mainland harbors (~30 cm) (Baptista and Miranda, 2009).

A common feature of most past large earthquakes is that they occurred offshore, in areas not covered by any type of detection instruments. Furthermore, the tsunami waves took only few tens of minutes to reach the closest coasts. IPMA (Instituto Português do Mar e da Atmosfera), as the Portuguese Agency responsible for seismic and tsunami monitoring, faces the challenge of using land-based seismometers providing less coverage of offshore earthquakes and tide gauges allowing to detect the tsunami only when they reach the coast. Yet, a unique opportunity is emerging to improve the earthquake and tsunami forecast capabilities in the NE Atlantic using the submarine cables that cross the main active tectonic areas and join Portugal mainland, Madeira and Azores archipelagos on a ring configuration. The current cables will cease their operation by 2024, 2025 and 2028 (due to the end of cable lifetime), and the process of their replacement by a new set of cables is now under consideration by the Portuguese authorities with the technical requirements to be defined in mid-2021. New developments in optical fiber cable technology allowing the use of existing telecommunication cables to provide seismic and tsunami information would be also beneficial to enhance the IPMA's monitoring network capabilities in the Atlantic Ocean.

The mitigation of the hazards posed by offshore earthquakes and tsunamis requires that the monitoring networks provide a timely and precise evaluation of the tectonic sources. There are considerable constraints and limitations when only land stations and coastal tide-gauges are used for the monitoring effort. In this work we show how submarine telecommunication cables can be used to improve the reliability of earthquake and tsunami monitoring. In *Earthquake and Tsunami Monitoring* we describe the current status of the seismic and tide-gauge monitoring networks and the procedures for issuing the first information message for the Civil Protection Agency. In *Optical Fiber Telecommunication Cable Technologies Available* we present briefly three available technologies to provide offshore monitoring services. In *Testing Scenarios* we define the testing scenarios and methodology to be used for each of the three cable technologies. In *Methods and Results* we present the simulation results and make a discussion and conclusions in *Discussion and Conclusions*.

Earthquake and Tsunami Monitoring

IPMA (Instituto Português do Mar e da Atmosfera) is the Portuguese Agency responsible for earthquake and tsunami monitoring and it has the responsibility to inform authorities as fast as possible on occurring earthquakes and possible tsunamis. For this purpose, IPMA is collecting seismic data from a dense network, exclusively based on land stations, many of them available through international cooperation (Figure 3) (Carrilho et al., 2021). Figure 3 also shows the location of the largest magnitude earthquakes that occurred in the offshore domain between Portugal mainland and the Azores, all of them having generated tsunamis. Given that there is no consensus on the source area for the Mw ~ 8.5 November 1st, 1755 earthquake and tsunami (Stucchi et al., 2013) we show on Figure 3 a series of tectonic structures that have been suggested by several authors as its possible source. Another earthquake that occurred close to the Azores, generating a small tsunami, is also mentioned (the Ms7.1 May 8th1939, Reis et al., 2017).
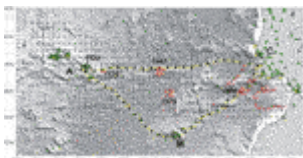
FIGURE 3

FIGURE 3. Hypothesized location of the submarine telecom cables that are expected to begin operation in 2024 in yellow. The black dots mark the presumed location of telecom repeaters, every 70 km spaced offshore, with the first repeater 40 km from the shoreline. The red stars show the epicenter location of the largest earthquakes that occurred in the area since 1940, 1941, 1975, and 1969. Several tectonic structures (in red) have been proposed SW Iberia as the source of the large earthquake and tsunami the November 1st, 1755. The smallest red star shows the location of the May 8th 1939 (Ms7.1) earthquake that caused a small tsunami recorded in several tide gauges in the Azores. Green triangles show the location of the land seismic stations used by IPMA for earthquake monitoring. PDa – Ponta Delgada tide gauge. Yellow triangles show the location of the coastal tide gauges that are monitored by IPMA for tsunami early warning. The white dots show the location of the tsunami sources in the IPMA scenario database, spaced every half a degree (Annunziato et al., 2009).

IPMA is collecting data continuously and seismic events are first detected and evaluated automatically and later on confirmed by an on-duty analyst covering 24/7. The analyst starts validating the phase picks and earthquake parameters as soon as 10 clear waveforms are received recording P-wave arrivals. The detection, classification and location of all offshore earthquakes is a continuous observation as the earthquakes evolves so that the source parameters can be updated in order to inform the local

authorities no later than 5 min after the event onset. This first information may be refined and updated afterwards when more data is analyzed by the analyst, but in this work, we focus on the quality of the earthquake parameters presented on this first message.

In parallel IPMA runs the Portuguese National Tsunami Warning Centre (PT.NTWC) which is in charge to issue to Civil Protection and authorities messages reporting the tsunami threat when a large offshore, or close to the shore, earthquake occurs. IPMA is also now recognized by the ICG-NEAMTWS (Intergovernmental Coordination Group for the Tsunami Early Warning and Mitigation System in the North-eastern Atlantic, the Mediterranean and connected seas) as an accredited International Tsunami Service Provider (TSP) responsible for tsunami information to the subscribing countries in the NE Atlantic. Both National and International systems operate under the same rules. As soon as the preliminary earthquake parameters are obtained in the 24/7 operational room, a decision matrix is applied to define the level of tsunami threat and the areas where such a level is applicable. The earthquake parameters required to apply the decision matrix are the epicenter location, magnitude and focal depth. The decision matrix was agreed by the ICG-NEAMTWS based on the best knowledge of past tsunamis in the NE Atlantic. It is a conservative rule that was established with the aim to avoid missing any possible tsunami. Considering this, linked to the uncertainty on the fast earthquake parameters, it is likely that the first message issued by this PT.NTWC/TSP (and others operating under the same rules) will give an alert level often exceeding the final observed tsunami waves. To better evaluate the tsunami threat sea-level observations are required. When these are made available, additional messages are sent updating the threat level and/or cancelling the tsunami alert. With only coastal tide-gauges available (Figure 3), considering also that some minutes are needed to measure the initial tsunami wave height (typically a quarter of a period), it is clear that large stretches of the coastline (those where the tsunami arrives first) will not benefit from the more reliable threat level evaluation given by these secondary messages (Omira et al., 2009).

Given that the most credible sources for large tsunamis lie offshore SW Iberia, Omira et al. (2009) showed, using tsunami simulations, that most on the southern coasts of Portugal do not benefit from enough warning time when the confirmation message is sent. These authors also showed the need to include offshore sea-level real-time measurements in the PT.NTWC/TSP to ensure that all Portugal would benefit from 10 min lead time before the first tsunami wave hits the shore.

The effectiveness and reliability of the earthquake and tsunami monitoring system, that must respond only a few minutes after the event onset, relies heavily on the geometry of the first seismic stations that are used for earthquake location, namely its geographical spreading and distance to the source. We show here two examples of location uncertainties and bias that result from a less than optimal station distribution. These examples reinforce the need for offshore sensors as the ones that can be provided by the fiber optic cable technologies discussed in this work.

From August 2007 to July 2008 a set of 24 broadband Ocean Bottom Seismometers (OBS) were deployed in the Gulf of Cadiz, SW Iberia, within the EU-funded NEAREST project (Integrated observations from NEARshore sourcES of Tsunamis: towards an early warning system) (Geissler et al., 2010). The OBS network revealed many earthquakes that were not previously recorded by the land network and its tectonic interpretation is provided in Silva et al. (2017). Geissler et al. (2010) used the 37 largest earthquakes recorded by the land network and relocated them with the OBS data. Using the information provided by Geissler et al. (2010) we make a graphical comparison between the epicenters and focal depths computed by the two networks, land and OBS. This comparison is shown in Supplementary Figure S1. The epicenters located with the land network are several km displaced to land, showing a systematic bias (bias = 17.5 ± 8.9 km). The largest difference between the two networks is found on the focal depth. OBS have shown that most local earthquakes are sourced in the upper mantle, tens of km deeper than the depth obtained from the land network (bias = 32 ± 11 km).

The July 9th, 1998 a strong earthquake (ML5.8, Mw6.1) struck the island of Faial causing 9 casualties, more than 150 people injured and the damaging of over 1,500 houses (Matias et al., 2007). This event was recorded by the Azores seismic network and also worldwide with several agencies providing estimates for epicenter, magnitude and focal mechanism in the few hours following the earthquake origin. Matias et al. (2007) show in their Figure 4a compilation of published parameter events and those from real-time services available on the Internet. This figure shows a very wide dispersion in the epicenter location that was interpreted as being a consequence of the absence of near-source seismic data. The closest station with data available by international agencies lied in S. Miguel Island, ~300 km away from the source.
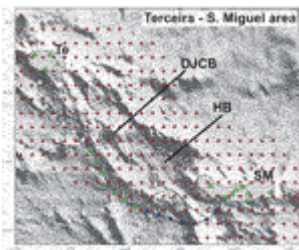
FIGURE 4

FIGURE 4. Layout of sensors and sources for the investigation of the DAS contribution to the monitoring of earthquakes in the Azores. Red dots show the epicenter synthetic locations, a regular grid with 0.1° interval. The green triangles on land show the existing seismic stations operated by IPMA. Black line is the presumed location of the Terceira-S. Miguel submarine cable, along which the colored triangles show the virtual seismic stations spaced every 10 km. The location strategy adopted considers the cable split into 3 segments that are identified with different colors. Te – Terceira Island, SM – S. Miguel Island, DJCB – D. João de Castro Bank, HB – Hirondelle Basin.

Optical Fiber Telecommunication Cable Technologies Available

Recent developments in optical fiber technology allows the use of existing and new submarine telecommunication cables to provide seismic and sea-level information crucial to monitor both earthquakes and tsunamis. In this work we study the potential impact of three different technologies, 1) SMART, Science Monitoring and Reliable Telecommunications; 2) DAS, Distributed Acoustic Sensing, and; 3) LI, Laser Interferometry, on the NE Atlantic earthquake and tsunami monitoring capabilities. From these technologies, only SMART can provide sea-level data to support the Tsunami Early Warning Systems.

Smart

SMART cables (Howe et al., 2019) are not yet implemented in any place on the world. There are already several dedicated submarine cables with geophysical sensors delivering essential data in real-time to the shore for early warning purposes in Japan (e.g., Okada et al., 2004), United States and Canada (e.g., Barnes et al., 2015; Trowbridge et al., 2019). However, this existing technology is not yet deployed on telecom submarine cables, as proposed by Howe et al. (2019). SMART sensors can only be installed on new submarine cables or reusing decommissioned telecom cables. The basic sensor package that is being proposed comprises ground motion sensors (seismometers, accelerometers or both), absolute pressure gauges for tsunami early warning and environmental monitoring, and one thermometer.

Das

DAS typically uses a single dedicated (dark) fiber on an installed submarine cable, with a length about ~70 km (although ranges up to 180 km have been mentioned). DAS technology uses optical time domain reflectometry based in Rayleigh or other backscattering effect to detect and localize discontinuities of optical fiber parameters along its length. Due to the backscattering along the fiber, the energy of a particular pulse of time duration T sent to the fiber is detected in the same sending side, as a received signal with time duration of the double of the travel time of the pulse along the fiber. Analyzing the received signal, associated with each sent pulse, with Digital Signal Processing it is possible to measure and define for each specific portion of the fiber (Gauge Length) the respective changes of the fiber strain, from sending pulse to sending pulse. The gauge Length is associated with the time interval T of the pulse sent. A DAS system can be modelled as a one dimensionally distributed fiber strain sensor, with localization ability (Gauge Length) down to some meters. DAS is nowadays a common tool on seismic exploration in the Oil and Gas industry and heavy civil construction infrastructures, being demonstrated its ability to record earthquakes with a resolution similar to broadband seismic sensors.

Li

In the seminal proof of concept of the method (Marra et al., 2018) the authors use a metrology grade frequency stabilized laser. The laser light is injected into the line as unmodulated sinusoidal carrier wave, with a carrier optical frequency stabilized to optical bandwidth of order 1 Hz. For telecom standards, this is an exceptional low value, albeit standard in time and frequency metrology instrumentation. It is more than a thousand times below state of the art telecom industry standards, including submarine links. The demonstration (Marra et al., 2018) used an optical back loop at the far side, where a radio-frequency modulation of an acoustic modulator was used to shift the optical carrier frequency. At the receptor side, the two light wave branches were interferometrically combined and detected and analyzed with RF techniques, and the optical phase shift monitored. The LI signal tracks the temporal changes of phase integrated over the whole link range. In bi-directional mode the arrival point of the first seismic waves can be determined and hence the system can be modeled as a distributed sensor. The traces of monitored optical phase shifts can then be compared with typical seismic traces. The proof of concept demonstration showed similarity when compared to seismic traces. LI may use a dedicated so-called dark fiber, or a single wavelength ITU

(International Telecommunication Union) channel in an optical fiber with commercial traffic co-existing on adjacent channels. The detection capability of LI probably will extend over the full range of the cable without length limitations.

Testing Scenarios

The Background Scenario

The monitoring of earthquakes and tsunamis done in real-time 24/7 by IPMA is exclusively based on land seismic stations and coastal tide-gauges (Figure 3). The contribution of submarine cables to this monitoring effort depends on the location of the seismic sources. We then investigate the added value of the three fiber optic technologies considering a regular set of tectonic sources encompassing the main seismically active domains along the Portugal mainland, Madeira and Azores regions.

At the largest scale we used the IPMA tsunami scenario database described in Annunziato et al. (2009). This database comprises a regular set of epicenters (considered as the center of the surface projection of the fault trace) that span the tectonically active areas and cover the main tsunamigenic sources identified (Figure 3) with 0.5° interval. At each epicenter the tsunami source considered is the worst case possible (pure dip slip events) with fault parameters as defined in Matias et al. (2013). The depth of the top of the fault is fixed to 5 km (worst case scenario) and magnitudes range from 6.5 to 8.75, spaced every 0.25. A total of ~7,000 scenarios was defined accordingly (~500 locations) and for each scenario the tsunami arrival time and tsunami amplitude at the coast (50 m depth) was numerically computed. The tsunami waveform at each coastal location can be obtained in real time by interpolation of the computed tsunami grids available every minute. The purpose of such tsunami scenario database was to help the tsunami warning system operator to define the threat level to be communicated to Civil Protection and authorities. The database is still used in training but not in the operational procedures, where the decision matrix is applied.

In the Azores this epicenter grid is too sparse, and we used another regular set of synthetic epicenters with a finer grid, appropriate to the known seismicity.

The Submarine Cable Scenarios

We consider that, whatever the fiber optic cable technology used, the cable can be represented by an additional set of seismic stations and sea-level sensors, contributing to the earthquake and tsunami monitoring like its land and coastal based counterparts, helping to constrain the offshore sources given their closer proximity.

SMART

In order to meet the low data latency, instrument location and spacing for an effective earthquake and tsunami early warning system we consider that the seismic and absolute pressure gauge sensors are positioned at the presumed locations of the cable repeaters. The closest repeaters to the shore are placed 40 km along the cable while the other sensors are regularly spaced with ~70 km interval. These locations are shown in Figure 3 for a presumed trajectory of the new CAM ring cables, to be operational in 2024.

DAS

We consider here that the maximum range of useful information by DAS is 100 km from the land station. This limits the usefulness of DAS in SW Portugal where the most credible sources for large earthquakes and tsunamis are offshore and most of them too distant from the presumed track of the new CAM ring cables (Figure 3). However, this technology may prove to be very useful in the Azores archipelago where most of the strongest earthquakes occur offshore, not very far from the Islands, and the seismic stations are concentrated on the Islands forming patches of sensors.

For this reason, we selected one of the most active areas in offshore Azores, the D. João de Castro Bank and Hirondelle Basin, one domain bordered by a submarine telecommunication cable between Terceira and S. Miguel Islands (Figure 2).

DAS can provide information on the strain rate along the cable with a gauge length as small as 10 m. For one monitoring length of 100 km, DAS provides information on 10,000 sensors, which is clearly in excess to what can be processed in the earthquake monitoring center. For this evaluation exercise we consider that DAS data is decimated in order to provide strain rate data on virtual sensors spaced 10 km along the cable (Figure 4). The cable layout shown is an estimate of the true cable positioning. The synthetic earthquake scenario comprises a regular grid of epicenters with 0.1° interval, spanning the recognized active area (Figure 4). As before, focal depth is fixed to 5 km.

LI

The laser interferometry technology as described in this work allows one to obtain the location of the point in the cable that the seismic waves hit first and the azimuth to the source waves, that must be orthogonal to the cable, with an ±180° ambiguity. This ambiguity can be easily solved in the operational room when more recordings from the land stations are available, or if another LI cable is operating nearby (e.g., Marra et al., 2018). The LI instrumented cable operates as one seismic station where the P-wave arrival time can be measured and where the cable to source azimuth can be also evaluated. However, this seismic station can be anywhere along the cable, depending on the relationship between the cable and the earthquake epicenter.

To evaluate the contribution of LI technology to the monitoring of earthquakes we consider that it can be replaced by a regular set of seismic stations (able to compute also the azimuth to the source) with a regular spacing of 8 km along the cable. This value exceeds the probable location uncertainty of the impact point on the cable, but it was found adequate for the following analysis. The longer the cable, the more advantageous will be the LI technology. Since the Azores – Madeira – Mainland is investigated using the SMART technology, we choose the Azores as the most interesting area to demonstrate the added value of LI. In the Azores, one of the longest cables is the one joining Faial and Flores Islands (Figure 2) 260 km long. It crosses the Mid-Atlantic Ridge plate boundary and borders by the south a very seismically active area, west of Faial, where several felt earthquakes have been generated in the past causing concern among the population and authorities. The total number of virtual seismic stations along the cable is 32. The experiment layout for LI is shown in Figure 5. The focal depth of the synthetic epicenter grid is fixed to 5 km.
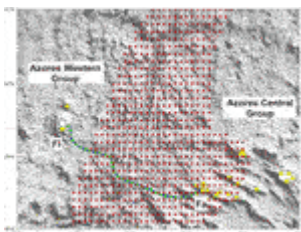
FIGURE 5

FIGURE 5. Layout of sensors and sources for the investigation of the LI contribution to the monitoring of earthquakes in the Azores. Red dots show the epicenter synthetic locations, a regular grid with 0.1° interval. The yellow triangles on land show the existing seismic stations operated by IPMA. Blue line is the presumed location of the Faial-Flores submarine cable, along which the green triangles show the virtual seismic stations spaced every 8 km. Fl – Flores Island, Fa – Faial Island.

Methods and Results

Tsunami Monitoring

Out of the three fiber optic technologies investigated in this work, only SMART sensors, measuring the absolute pressure with high resolution (by an APG), can provide offshore real-time data as required for an effective PT.NTWC/TSP. In Howe et al.[1] (submitted) we find the gain in warning time that a set of sensors deployed along the cables Mainland-Madeira and Mainland-Azores can provide. This is a simple consequence of the geometry of the offshore APGs and required only the computation of the minimum tsunami travel time to the land based, or cable based, sensor networks.

In addition to the gain on the minimum-tsunami detection time, we believe that the proposed cabled sensors will allow improving the performance of the PT.NTWC through recording tsunami signals of better quality than the ones typically recorded by the coastal tide gauge (CTG) network. The preparation of the tsunami confirmation messages by the PT.NTWC operator requires the identification and measurement of tsunami wave characteristics (arrival time, wave height, and period). Sometimes, this task is hard to perform due to the quality of the sea-level signal at CTG that usually includes the tidal variation and is contaminated by coastal effects, involving noise able to mask the tsunami signal. Any additional treatment of the sea-level record to isolate the tsunami signal (quality control, de-tiding and noise removing) before measuring the waves characteristics may consume critical operator time. The presence of cabled sensors will allow overcoming this limitation as they will offer the possibility to record the tsunami in the open ocean without the coastal effects. To explore such a benefit, we present a numerical tsunami propagation scenario involving a Mw8.3 earthquake similar to the 1941 strike-slip event that took place on the Gloria Fault (Omira et al., 2019). The tsunami numerical simulation is performed using a validated non-linear shallow water code in the presence of both offshore geophysical repeaters (cabled sensors) and coastal tide gauges (Figure 6A). Synthetic sea-level records at both the costal tide gauge of Ponta Delgada (Figure 6B) and the cabled sensor GR-8 (Figure 6C) are then compared. The comparison clearly shows that the cabled sensor allows a fast confirmation of tsunami occurrence and an easy measurement of the wave characteristics (wave arrival, height and period) required to update the tsunami alert messages.
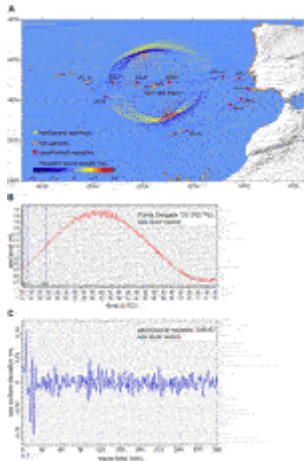
FIGURE 6

FIGURE 6. Sea-level signal quality comparison. **(A)** tsunami numerical propagation for a 1941-like earthquake in the presence of cabled sensors and tide gauge stations **(B)** signal recorded at the Ponta Delgada tide gauge; **(C)** signal recorded by a cabled sensor (GR-8 in a). OT = earthquake origin time.

It is also worth mentioning that the installation of sensors in the submarine cable can significantly boost the development of the next-generation TWS in the NE Atlantic. Integrating rapid offshore tsunami observations and advanced tsunami numerical models is crucial to develop real-time and reliable tsunami forecasting (Titov et al., 2005). The Pacific TWS inverses the offshore tsunami signals (from oceanic buoys) to determine the earthquake-induced initial sea surface perturbation. This latter is then used as initial condition for "faster-than-real-time" numerical code enabling to predict the tsunami threat on the coast. The implementation of such a methodology in the NE Atlantic TWS would be possible with the presence of cabled sensors allowing early and high-quality tsunami observations. Offshore real-time sea level measurements may also provide early warning for non-tectonic tsunami sources like submarine landslides.

Earthquake Monitoring

The quality of the fast-computed earthquake parameters that are used for alerting Civil Protection is critically dependent on the geometry of the seismic network and its relationship with the source location. In Howe et al. (submitted) we examined the added value of cabled sensors using the SMART technology on 2 geometric parameters: 1) the maximum azimuthal gap between epicenter and recording stations; 2) the geometrical quality defined by Bondár and McLaughlin (2009) that takes also into consideration the regularity of the azimuth distribution. We also computed the gain in earthquake warning time which is a parameter that only depends on the network geometry (Howe et al., submitted). This parameter is most relevant for the performance of an Earthquake

Early Warning System (EEWS) which is planned but not yet operational in Portugal. The great improvement on the performance of one EEWS in Portugal demonstrated in Howe et al. (submitted) will not be further discussed in the present work.

These geometrical parameters, though relevant, cannot make a realistic assessment of the uncertainty that arises while determining earthquake parameters from a limited set of P-wave readings poorly located, either for the stations being far from the source or for them being too close together. In this work we present and apply Monte-Carlo simulations that take into consideration the errors in phase picking and the level of uncertainty on the velocity model used to compute the theoretical phase arrival times for a more representative evaluation of earthquake parameter uncertainties.

The Monte-Carlo Approach

We use 100 simulations of a synthetic set of phase readings computed with a velocity model that is altered from the used after for earthquake location. The location code is Hypocenter (Lienert et al., 1986), included in the seismic analysis tool SEISAN (Havskov et al., 2020). This is the same routine that IPMA uses in the seismic operational room. It uses a 1D velocity model that is changed according to the domain where the epicenter is found. These 1D models were obtained from published geophysical studies and they should represent an average of the velocity structure in each domain. However, the earth structure is not 1D.

To make a 1st order account for the 3D nature of the Earth in the AZGFZ area, IPMA uses in earthquake location different 1D models according to the earthquake epicenter (see Custódio et al., 2015, Figure 3). The models that apply to Portugal margins and the Gulf of Cadiz, to the oceanic domain to the West up to the Azores Archipelago, and to the Azores platform are shown in Supplementary Figure S2. The IPMA models are compared to two local models derived for detailed studies, Geissler et al. (2010) in the Gulf of Cadiz et al. (2007) in the Central Group of the Azores, showing the heterogeneity of the area at different scales. It was not the purpose of the present investigation to check if a 3D velocity model was more appropriate than 1D models for earthquake location. Instead, we wanted to explore the performance of cabled and not cabled seismic networks when a change in the "true" 1D velocity is considered. For this purpose, we used the IPMA "Margin" model to investigate the CAM geometry and used the IPMA "Azores" model to investigate the contributions of DAS and LI to earthquake location.

Starting with the "true" location on the synthetic catalogue, each Monte-Carlo (MC) simulation begins by defining one set of phase arrivals considering two types of random fluctuations: 1) P-wave phase picks are changed by a Gaussian random error with SD 0.2 s; 2) the velocity model is also modified by a Gaussian random perturbation. The velocity values are modified with 10% SD and the layer depths are changed by 1 km SD. These may be considered conservative values since we expect larger differences on the average velocity model the further away the station is from the epicenter.

Each MC simulation results into a set of earthquake location parameters computed with slightly different input parameters. Taken together, the 100 simulations can be used to assess the earthquake parameter uncertainty for a given network geometry, land stations only or land plus cabled sensors, for a set of synthetic locations regularly spaced. We translate this variability in a geographical grid using two quality parameters: 1) DD – the distance between the MC epicenter centroid and its true location; b) SS one length parameter equal to the square root of the area of the uncertainty ellipse defined by the covariance of the 100 simulations, $SS = \sqrt{s_1 s_2}$ SS=s1s2 where s_1, s_2 s1, s2 are the eigen values of the covariance matrix on the epicenter latitude and longitude measured in km. SS represents the radius of the circle that has the same area as the epicenter uncertainty ellipse. This is easier to interpret than using s_1 s1 or s_2 s2 since the ellipses are usually very elongated on one direction due to the geometrical constrains of the observation networks.

SMART

The added value of the SMART cable to earthquake monitoring is presented here considering the domain between Portugal mainland and the Azores, as displayed in Figure 3. This figure also shows the synthetic epicenter grid that will be used in the evaluation. The background scenario was computed considering that the fast earthquake parameters are obtained with the first 10 P-wave arrivals recorded on the land stations that were presented in Figure 3.

Figure 7A shows the comparison of the centroid location from the 100 MC simulations and the true synthetic catalogue. From the 100 locations on each synthetic epicenter we compute the covariance matrix of the epicenter coordinates to define an uncertainty ellipse. This ellipse and all epicenters are displayed in Figure 7C. These two plots show sharp transitions on these two quality parameters that are related to the geographical distribution of stations that are used for each location. The wider this distribution, the better constrained is the MC epicenter.
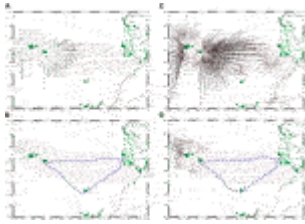
FIGURE 7

FIGURE 7. Visual comparison of Monte-Carlo quality earthquake location parameters when the synthetic catalogue is analyzed by the land only seismic station network (LAND, green triangles) or analyzed by the land and cabled (CABLE, blue triangles). **(A)** Distance between the MC centroid (in red) and the true location (in green) for LAND. **(B)** Distance between the MC centroid (in red) and the true location (in green) for CABLE. **(C)** All MC epicenters computed, and the uncertainty ellipse computed from the covariance of the horizontal coordinates for LAND. **(D)** All MC epicenters computed, and the uncertainty ellipse computed from the covariance of the horizontal coordinates for CABLE.

The contribution of the SMART cable to earthquake monitoring is evaluated using the cabled sensors presented in Figure 3 on all 3 branches. The same operational procedure is used here, the epicenters are computed using the first 10 stations (on land or on the cable) to record the P-wave arrival. When we began evaluating the results, we noted that quite a few of the offshore events were very poorly located by the "land pluscabled" network when only cabled sensors were used for the 10 first recordings. This is easy to explain since the cabled sensors are deployed along the linear cable which is a very poor distribution for stations to compute earthquake parameters. This is a problem, poor azimuthal coverage of the first 10 stations, that is already found by IPMA in the Azores, where the stations are concentrated on the Islands forming an E-W elongated archipelago. When a poorly constrained geometry is identified by the operator, it is decided to force the analysis to use data from close by Islands. A similar procedure was used here to mitigate the problem of having a large number of stations located along a line.

We split the cable into its 3 branches, CM, CA and MA, and forced the location algorithm to use at least one station from 4 groups of stations, 3 cabled plus the land network. Figures 7B and 7D display for the MC simulation of "land plus cabled" network locations respectively the comparison between centroid and true location (used to define the DD quality parameter) and the uncertainty location ellipses (used to compute the SS quality parameter). When compared to the land only results, a general improvement on the earthquake locations is observed when using the cabled sensors. There remain a few outliers, most of them at the border of the area investigated by the synthetic catalogue hinting that additional operational rules might need to be considered to address these particular events.

To quantify the added value of the SMART cable we built geographical grids with the DD and SS quality parameters previously defined. The gain in DD and SS obtained by the SMART cable is shown in Figure 8. The largest improvement on DD, the distance between the true epicenter location and the MC centroid is observed East of the Azores Archipelago, up to 21°W. East of 21°W the gain in DD is smaller, with some patches showing no improvement and others showing an improvement up to 40 km.
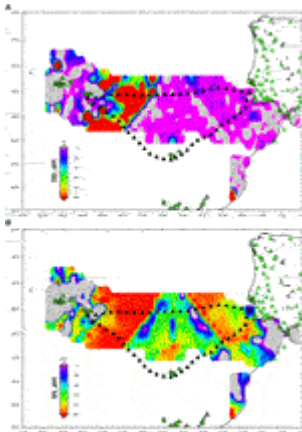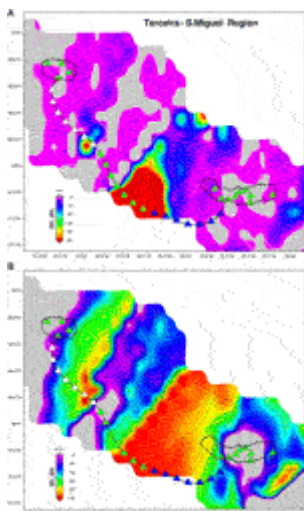
FIGURE 8

FIGURE 8. Measure of the added value of the SMART cables to the earthquake fast parameter determination using Monte-Carlo simulations. Green triangles show the land seismic stations while the cabled stations are shown as blue triangles. **(A)** Difference between "land plus cabled" and land only networks for the DD quality parameter. **(B)** Difference between "land plus cabled" and land only networks for the SS quality parameter, in %. On both images red areas show the domains were the difference is less than the maximum value, light grey areas show the domains were no improvement was observed.

The added value of the SMART cable is more evident when we consider the reduction in the length parameter SS shown in Figure 8B. All domain between the Azores and 8°W is benefited with a gain in SS that attains 100% or more. There is a triangular shape north of Madeira where the reduction in SS is smaller but still very significant, larger than 40%. The Azores Archipelago is not covered by cabled sensors and consequently there is no gain in most of the region. There is no gain also east of 8°W because the contribution of the cabled sensors is done by stations that are very far away.

DAS

The layout of the experiment designed to evaluate the added value of DAS to earthquake monitoring was explained in *Testing Scenarios*. Station distribution and synthetic epicentres are shown in Figure 4. We consider that one event is ready for location as soon as the P-wave reaches the 10 closest stations. For offshore events this may result in poor locations when all these stations are the cable sensors that are located along a line with bad azimuthal coverage. For this reason, we split the full set of sensors into 5

groups, one for each island and the cable split into 3 additional groups (Figure 4). The location is done only when at least one station from each group is included in the first 10 stations. Later P-wave arrivals are discarded until this condition is met. The background scenario comprises the land stations only.

Supplementary Figures S3A shows the comparison of the centroid location from the 100 MC simulations and the true synthetic catalogue for the background scenario. For this scenario, the uncertainty ellipse computed from the covariance matrix of the epicenter coordinates is displayed in Supplementary Figure S3C. The same parameters for the "land plus cabled" scenario are shown in Supplementary Figures S3B,D.

The added value of the DAS is better expressed by comparing the geographical grids built with the DD and SS quality parameters, as shown in Figure 9. The gain in DD (Figure 9A) is small in most of the domain investigated, less than 10 km or absent. The larger difference (greater than 10 km) is obtained West and NW of S. Miguel Island, with maximum decreases in DD larger than 50 km.

FIGURE 9

FIGURE 9. Measure of the added value of the DAS to the earthquake fast parameter determination using Monte-Carlo simulations. Green triangles show the land seismic stations while the cabled stations are shown as blue triangles. **(A)** Difference between "land plus cabled" and land only networks for the DD quality parameter. **(B)** Difference between "land plus cabled" and land only networks for the SS quality parameter, in %. On both images red areas show the domains were the difference is less than the maximum value, light grey areas show the domains were no improvement was observed.

The gain in SS (measuring the MC uncertainty ellipse area) is more widespread over the whole offshore domain investigated between S. Miguel and Terceira Islands (Figure 9B). The % decrease in SS in larger than 50% in most areas, except for one transversal

domain, closer to Terceira Island. The sharp transition in SS values observed is a natural consequence of the geometry of the network and the resulting choice of the 10 best stations to use for the fast earthquake parameter determination.

LI

The LI experiment was presented in *Testing Scenarios* and the layout of seismic stations and synthetic epicenters was shown in Figure 5. As before, we consider that the first earthquake location is obtained when 10 P-wave arrivals are recorded. The cable LI counts as a unique station that has two properties, it can be anywhere in the cable (split into 8 km sections) and that station, besides the phase arrival time, can provide the station to azimuth angle. The 180° ambiguity can be easily sorted out on the operation room. In the process of selecting the 10 stations used for computation we discard the LI stations that are closest to the shore. We consider that, for those locations, the azimuth is unreliable because the seismic waves can be originated from any location to the East or West of the cable. It is clear that the LI cable will improve the fast earthquake location if and only if one of the virtual cable locations is used.

Supplementary Figure S4A shows the comparison of the centroid location from the 100 MC simulations and the true synthetic catalogue for the background scenario. For this scenario, the uncertainty ellipse computed from the covariance matrix of the epicenter coordinates is displayed in Supplementary Figure S4C. The same parameters for the "land plus cabled" scenario are shown in Supplementary Figures S4B,D.

By gridding DD and SS for the two scenarios, we can measure the gain provided by LI on a geographical grid. The gains obtained are shown in Figures 10A,B for DD and SS respectively. The comparison between MC centroids and the true synthetic location shows that LI improves significantly on a small domain in the middle of the LI cable. The remaining area investigated shows only a small improvement (less than 10 km) or no gain at all. The patchy pattern observed is a consequence of the MC simulations with random stochastic variations. Two runs of 100 simulations will not be identical even if using the same set of stations.
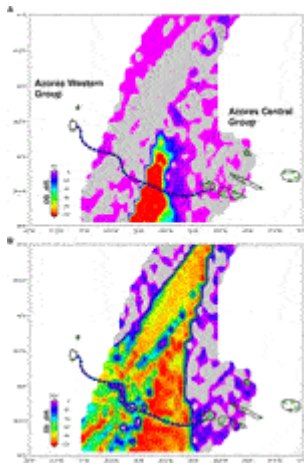
FIGURE 10

FIGURE 10. Measure of the added value of the LI cable to the earthquake fast parameter determination using Monte-Carlo simulations. Green triangles show the land seismic stations while the cabled stations are shown as blue triangles. **(A)** Difference between "land plus cabled" and land only networks for the DD quality parameter. **(B)** Difference between "land plus cabled" and land only networks for the SS quality parameter, in %. On both images red areas show the domains were the difference is less than the maximum value, light grey areas show the domains were no improvement was observed.

On the other hand, the comparison of the uncertainty ellipse area, SS shown in Figure 10B, displays a considerable gain obtained by the LI cable on a large triangular domain with one vertex to the NE of the cable. This triangular shape illustrated the source domain where one LI cable station contributes to the earthquake location. When that happens, the knowledge of one additional P-wave arrival and the azimuth from station to event improves significantly the fast determination of earthquake parameters, essential for Civil Protection authorities. One single station could make a huge difference.

Discussion and Conclusions

Fiber optic submarine cables that are used for telecommunications provide nowadays two technologies that can be used for the improvement of offshore earthquake and tsunami monitoring: 1) SMART – the deployment of geophysical sensors on new cables (Howe et al., 2019); 2) DAS – recording fiber strain rate on existing (or new) dark fibers (e.g., Fernández-Ruiz et al., 2020). One emerging technology, LI, is based on ultra-stable laser interferometry, it can be used on existing cables, doesn't need a dark fiber to be applied, and shows high potential for real-time measurements of strain rate along the fiber (Marra et al., 2018). In this work we explored and quantified the contributions that each of the three technologies could bring to the earthquake monitoring effort along the Azores-Gibraltar plate boundary, a very active domain responsible for the largest earthquake in Europe since year 1000 (Stucchi et al., 2013). As regards tsunami observation, only SMART cables can provide sea-level observations on the open ocean, as required by a fast and reliable evaluation of the tsunami threat level.

Our exercise was based on the standard operation routines at IPMA, the Portuguese agency responsible for the earthquake monitoring in this domain, namely that the first message to be issued to authorities has to be delivered in less than 5 min after the event

onset. The operator starts the validation of the automatic picking and earthquake parameter computation as soon as 10 P-wave arrivals are received. The quality of these first parameters is strongly dependent on the geometry of the 10 stations that are used for the location. Tsunami waves can only be currently observed by coastal tide gauges and the update of tsunami information will not benefit the coasts that are hit first.

The changes in parameters that depend exclusively on the geometry of the network, maximum azimuthal gap between recording stations, the U parameter defined by Bondár and McLaughlin (2009), the time needed to reach the minimum number of seismic stations for Earthquake Early Warning, the time needed to reach the first sea-level sensor used for Tsunami Early Warning, are presented in Howe et al. (submitted). In this work we proposed to go one step further from simple geometrical considerations.

Considering tsunamis, we showed how the detection of changed sea-level is much faster and simpler in offshore sensors than in coastal tide-gauges, opening the opportunity for assessing the tsunami threat by numerical modeling, before the waves arrive to the coast.

As regards earthquake monitoring, we concentrated our efforts on the gain that cable sensors can provide to the very first information that is communicated to the authorities based on the first 10 P-wave readings that are recorded by the seismic network. The earthquake location is then derived using an appropriate 1D velocity model. Two sources of errors contribute to the uncertainty on the epicenter location, an ambiguity in the P-wave reading and the inadequacy of the velocity model to simulate the wave propagation on a 3D Earth structure. We used 100 Monte-Carlo simulations to assess the variability on the epicenter computation that results from these two sources of uncertainty. Two MC quality parameters were considered: DD – the distance between the MC centroid of epicenters and the true location defined on a synthetic catalogue; SS – the square root of the area of the uncertainty ellipse as defined by the covariance matrix of the epicenter coordinates. Since the cabled sensors are aligned along the linear submarine cable, they are not very helpful, due to its poor azimuthal coverage, if they are the only sensors used for earthquake location. For this reason, we devised a strategy for the choice of the 10 stations to be used for the fast earthquake parameter determination, that can be easily implemented in the operational room taking the IPMA practice in the Azores as an example.

When comparing the background scenario (land stations only) with the improved scenario (land plus cabled network) we observed that the comparison of MC centroid locations was not very helpful to bring out the added value of the cable technologies. The

centroid is an average and it seems that, with the simulation parameters used, in many domains, the land only network is able to recover the true epicenter on average. However, in real life we don't have 100 repetitions of each event. We showed that, despite DD being small, the uncertainty on epicenter determination as measured by SS is large or very large when land stations only are used. All 3 technologies investigated, SMART, DAS and LI showed very significant reduction on the epicenter uncertainty in the offshore domains that are known to be able to generate strong earthquakes and tsunamis.

The added value provided by instrumented submarine telecommunication cables to mitigate earthquake and tsunami risk that is demonstrated in this work may help authorities and the society in general to take the political decisions required for its full implementation.

Data Availability Statement

The original contributions presented in the study are included in the article/Supplementary Material, further inquiries can be directed to the corresponding author.

Author Contributions

LM wrote the 1st version of the manuscript with input from all authors. All authors made substantial contributions to the overall science case and manuscript and approved it for publication. RO and FC drafted the tsunami monitoring case. LM, FC, and CC drafted the earthquake monitoring case. VS, MN, and YO drafted the DAS and LI cases. JB contributed the manuscript ideas and for the references calling the attention for the need of having political decisions.

Funding

Conflict of Interest

The authors declare that the research was conducted in the absence of any commercial or financial relationships that could be construed as a potential conflict of interest.

Acknowledgments

Supplementary Material

The Supplementary Material for this article can be found online at: https://www.frontiersin.org/articles/10.3389/feart.2021.686296/full#supplementary-material

Footnotes

[1]Howe, B., Angove, M., Arcas, D., Aucan, J., Barnes, C. R.,Barros, J., et al. (2020). SMART Subsea Cables for Observing the Earth and Ocean: Update. Front. Mar. Sci.

References

Annunziato, A., Carrilho, F., Matias, L., Baptista, M. A., and Omira, R. (2009). Progresses in the Establishment of the Portuguese Tsunami Warning System. *EMSC Newsletter*, 10–12. April.

Google Scholar

Baptista, M. A., Miranda, J. M., Batlló, J., Lisboa, F., Luis, J., and Maciá, R. (2016). New Study on the 1941 Gloria Fault Earthquake and Tsunami. *Nat. Hazards Earth Syst. Sci.* 16, 1967–1977. doi:10.5194/nhess-16-1967-2016

CrossRef Full Text | Google Scholar

Baptista, M. A., and Miranda, J. M. (2009). Revision of the Portuguese Catalog of Tsunamis. *Nat. Hazards Earth Syst. Sci.* 9, 25–42. doi:10.5194/nhess-9-25-2009

CrossRef Full Text | Google Scholar

Barnes, C. R., Best, M. M. R., Johnson, F. R., and Pirenne, B. (2015). "NEPTUNE Canada: Installation and Initial Operation of the World's First Regional Cabled Ocean Observatory," in *In Seafloor Observatories: A New Vision of Earth from the Abyss*. Editors A. De Santis, P. Favali, and L. Beranzoli (Berlin: Springer-Verlag Berlin Heidelberg), 415–438. doi:10.1007/978-3-642-11374-1_16

CrossRef Full Text | Google Scholar

Bird, P. (2003). An Updated Digital Model of Plate Boundaries. *Geochem. Geophys. Geosyst.* 4, 1027. doi:10.1029/2001gc000252

CrossRef Full Text | Google Scholar

Bird, P., and Kagan, Y. Y. (2004). Plate-tectonic Analysis of Shallow Seismicity: Apparent Boundary Width, Beta, Corner Magnitude, Coupled Lithosphere Thickness, and Coupling in Seven Tectonic Settings. *Bull. Seismological Soc. America* 94, 2380–2399. doi:10.1785/0120030107

CrossRef Full Text | Google Scholar

Bondár, I., and McLaughlin, K. L. (2009). A New Ground Truth Data Set for Seismic Studies. *Seismological Res. Lett.* 80, 465–472. doi:10.1785/gssrl.80.3.465

CrossRef Full Text | Google Scholar

Carrilho, F., Custódio, S., Bezzeghoud, M., Oliveira, C. S., Marreiros, C., Vales, D., et al. (2021). The Portuguese National Seismic Network-Products and Services. *Seismological Res. Lett.* 92, 1541–1570. doi:10.1785/0220200407

CrossRef Full Text | Google Scholar

Custódio, S., Dias, N. A., Carrilho, F., Góngora, E., Rio, I., Marreiros, C., et al. (2015). Earthquakes in Western Iberia: Improving the Understanding of Lithospheric Deformation in a Slowly Deforming Region. *Geophys. J. Int.* 203 (1), 127–145. doi:10.1093/gji/ggv285

CrossRef Full Text | Google Scholar

Fernandes, R. M. S., Miranda, J. M., Meijninger, B. M. L., Bos, M. S., Noomen, R., Bastos, L., et al. (2007). Surface Velocity Field of the Ibero-Maghrebian Segment of the Eurasia-Nubia Plate Boundary. *Geophys. J. Int.* 169, 315–324. doi:10.1111/j.1365-

246x.2006.03252.x

CrossRef Full Text | Google Scholar

Fernández-Ruiz, M. R., Soto, M. A., Williams, E. F., Martin-Lopez, S., Zhan, Z., Gonzalez-Herraez, M., et al. (2020). Distributed Acoustic Sensing for Seismic Activity Monitoring. *APL Photon.* 5, 030901. doi:10.1063/1.5139602

CrossRef Full Text | Google Scholar

Geissler, W. H., Matias, L., Stich, D., Carrilho, F., Jokat, W., Monna, S., et al. (2010). Focal Mechanisms for Sub-crustal Earthquakes in the Gulf of Cadiz from a Dense OBS Deployment. *Geophys. Res. Lett.* 37, n/a. doi:10.1029/2010GL044289

CrossRef Full Text | Google Scholar

Gutenberg, B., and Richter, C. F. (1949). *Seismicity of the Earth and Associated Phenomena*. Princeton, New Jersey: Princeton University Press, 273.

Havskov, J., Voss, P. H., and Ottemöller, L. (2020). Seismological Observatory Software: 30 Yr of SEISAN. *Seismological Res. Lett.* 91, 1846–1852. doi:10.1785/0220190313

CrossRef Full Text | Google Scholar

Hirn, A., Haessler, H., Trong, P. H., Wittlinger, G., and Victor, L. A. M. (1980). Aftershock Sequence of the January 1st, 1980, Earthquake and Present-Day Tectonics in the Azores. *Geophys. Res. Lett.* 7, 501–504. doi:10.1029/gl007i007p00501

CrossRef Full Text | Google Scholar

Howe, B. M., Arbic, B. K., Aucan, J., Barnes, C. R., Bayliff, N., Becker, N., et al. on behalf of the Joint Task Force for SMART Cables (2019). SMART Cables for Observing the Global Ocean: Science and Implementation. *Front. Mar. Sci.* 6, 424. doi:10.3389/fmars.2019.00424

CrossRef Full Text | Google Scholar

Johnston, A. C. (1996). Seismic Moment Assessment of Earthquakes in Stable continental Regions-III. New Madrid 1811-1812, Charleston 1886 and Lisbon 1755. *Geophys. J. Int.* 126, 314–344. doi:10.1111/j.1365-246x.1996.tb05294.x

CrossRef Full Text | Google Scholar

Kanamori, H., and Abe, K. (1979). Reevaluation of the Turn-Of-The-Century Seismicity Peak. *J. Geophys. Res.* 84 (B11), 6131. doi:10.1029/JB084iB11p06131

CrossRef Full Text | Google Scholar

Lienert, B. R., Berg, E., and Frazer, L. N. (1986). HYPOCENTER: An Earthquake Location Method Using Centered, Scaled, and Adaptively Damped Least Squares. *Bull. Seismological Soc. Am.* 76, 771–783. doi:10.1785/bssa0760030771

CrossRef Full Text | Google Scholar

Marra, G., Clivati, C., Luckett, R., Tampellini, A., Kronjäger, J., Wright, L., et al. (2018). Ultrastable Laser Interferometry for Earthquake Detection with Terrestrial and Submarine Cables, 361, 486–490. doi:10.1126/science.aat4458

CrossRef Full Text | Google Scholar

Martinez-Solares, J. M., and Lopez-Arroyo, A. (2004). The Great Historical 1755 Earthquake. Effects and Damage in Spain. *J. Seismology* 8, 275–294. doi:10.1785/bssa0760030771

CrossRef Full Text | Google Scholar

Matias, L., Dias, N. A., Morais, I., Vales, D., Carrilho, F., Madeira, J. L., et al. (2007). The 9th of July 1998 Faial Island (Azores, North Atlantic) Seismic Sequence. *J. Seismol* 11, 275–298. doi:10.1007/s10950-007-9052-4

CrossRef Full Text | Google Scholar

Matias, L. M., Cunha, T., Annunziato, A., Baptista, M. A., and Carrilho, F. (2013). Tsunamigenic Earthquakes in the Gulf of Cadiz: Fault Model and Recurrence. *Nat. Hazards Earth Syst. Sci.* 13, 1–13. doi:10.5194/nhess-13-1-2013

CrossRef Full Text | Google Scholar

Okada, Y., Kasahara, K., Hori, S., Obara, K., Sekiguchi, S., Fujiwara, H., et al. (2004). Recent Progress of Seismic Observation Networks in Japan -Hi-Net, F-Net, K-NET and KiK-Net-. *Earth Planet. Sp* 56, xv–xxviii. doi:10.1186/bf03353076

CrossRef Full Text | Google Scholar

Omira, R., Baptista, M. A., Matias, L., Miranda, J. M., Catita, C., Carrilho, F., et al. (2009). Design of a Sea-Level Tsunami Detection Network for the Gulf of Cadiz. *Nat. Hazards Earth Syst. Sci.* 9, 1327–1338. doi:10.5194/nhess-9-1327-2009

CrossRef Full Text | Google Scholar

Omira, R., Neres, M., and Batista, L. (2019). The Gloria Transform Fault-NE Atlantic: Seismogenic and Tsunamigenic Potential. *Transform Plate Boundaries and Fracture Zones*, Elsevier, chap. 8, 157–167. doi:10.1016/b978-0-12-812064-4.00008-6

CrossRef Full Text | Google Scholar

Reis, C., Omira, R., Matias, L., and Baptista, M. A. (2017). On the Source of the 8 May 1939 Azores Earthquake–Tsunami Observations and Numerical Modelling. *Geomatics Nat. Haz. Risk,* 8 (2), 328–347. doi:10.1080/19475705.2016.1218944

CrossRef Full Text | Google Scholar

Silva, S., Terrinha, P., Matias, L., Duarte, J. C., Roque, C., Ranero, C. R., et al. (2017). On the Source of the 8 May 1939 Azores Earthquake - Tsunami Observations and Numerical Modelling. *Geomatics, Nat. Hazards Risk* 8, 226–241. doi:10.1080/19475705.2016.1218944

CrossRef Full Text | Google Scholar

Smith, W. H. F., and Sandwell, D. T. (1997). Global Sea Floor Topography from Satellite Altimetry and Ship Depth Soundings. *Science* 277, 1956–1962. doi:10.1126/science.277.5334.1956

CrossRef Full Text | Google Scholar

Stucchi, M., Rovida, A., Gomez Capera, A. A., Alexandre, P., Camelbeeck, T., Demircioglu, M. B., et al. (2013). The SHARE European Earthquake Catalogue (SHEEC) 1000-1899. *J. Seismol.* 17, 523–544. doi:10.1007/s10950-012-9335-2

CrossRef Full Text | Google Scholar

Titov, V. V., Gonzalez, F. I., Bernard, E. N., Eble, M. C., Mofjeld, H. O., Newman, J. C., et al. (2005). Real-time Tsunami Forecasting: Challenges and Solutions. *Nat. Hazards* 35, 35–41. doi:10.1007/s11069-004-2403-3

CrossRef Full Text | Google Scholar

Trowbridge, J., Weller, R., Kelley, D., Dever, E., Plueddemann, A., Barth, J. A., et al. (2019). The Ocean Observatories Initiative. *Front. Mar. Sci.* 6. doi:10.3389/fmars.2019.00074

CrossRef Full Text | Google Scholar

*Correspondence: Luis Matias, **lmatias@fc.ul.pt**

Disclaimer: All claims expressed in this article are solely those of the authors and do not necessarily represent those of their affiliated organizations, or those of the publisher, the editors and the reviewers. Any product that may be evaluated in this article or claim that may be made by its manufacturer is not guaranteed or endorsed by the publisher.